TOPICAL REVIEW • OPEN ACCESS

Unidirectional spin-wave propagation and devices

To cite this article: Jilei Chen *et al* 2022 *J. Phys. D: Appl. Phys.* **55** 123001

View the article online for updates and enhancements.

Topical Review

Unidirectional spin-wave propagation and devices

Jilei Chen[1,*] ⓘ, Haiming Yu[2,*] ⓘ and Gianluca Gubbiotti[3,*] ⓘ

[1] Shenzhen Institute for Quantum Science and Engineering, Southern University of Science and Technology, Shenzhen 518055, People's Republic of China
[2] Fert Beijing Institute, MIIT Key Laboratory of Spintronics, School of Integrated Circuit Science and Engineering, Beihang University, Beijing 100191, People's Republic of China
[3] Istituto Officina dei Materiali del CNR (CNR-IOM), c/o Dipartimento di Fisica e Geologia, Università di Perugia, I-06123 Perugia, Italy

E-mail: chenjl6@sustech.edu.cn, haiming.yu@buaa.edu.cn and gubbiotti@iom.cnr.it

CrossMark

Abstract

Unidirectional information transport plays a key role in optics, microwave technology, electronic logic circuits and devices. Spin waves (SWs) are considered to be a promising candidate for the next-generation logic devices, which have many advantages such as low-energydissipation and compatibility with radio-frequency-based electronic devices. Unidirectional SWs have been demonstrated in magnetic thin films theoretically and experimentally, offering a great opportunity to realize unidirectional transport of spin information. In this article, we review several methods for emitting and measuring unidirectional SWs, such as using the nonreciprocity provided by magnetostatic surface SWs and interfacial Dzyaloshinskii–Moriya interactions. Unidirectional SWs can also be excited by magnetic nanowire arrays as well as spatially defined spin textures. Finally, we review some magnonic logic devices based on unidirectional SWs, such as spin-wave diodes.

Keywords: magnonics, spin waves, unidirectionality

(Some figures may appear in colour only in the online journal)

1. Introduction

Spin waves (SWs), or their quanta magnons, are a collective precession of electron spins and they can propagate in magnetic systems without the motion of electrons [1–11]. The field of magnonics, which uses SWs to carry and process information, has recently seen rapid growth due to the promising future of low-energy-dissipation SW devices. Functioning from GHz to THz, SWs have four to five orders of magnitude smaller wavelengths than microwaves at the same frequency, which makes them compatible with modern nanoscale electronic devices and circuits [12–23].

Unidirectional transport of information plays a key role in optics [24–26], microwave technology [27] and electronics [28]. An optical isolator, or optical diode, is an optical component that allows the transmission of light in only one direction [29, 30]. It is typically used to ward off unwanted retrore-flections in an optical oscillator, such as a laser cavity.

In microwave technology, unidirectional devices such as filters, isolators, and circulators are based on gyrotropic properties of magnetization precession [31, 32]. These are macroscopic devices (typically of mm size), whereas advances in nanotechnology and understanding of

* Authors to whom any correspondence should be addressed.

magnetization dynamics in nanostructured materials permit the realization of nanoscale unidirectional and nonreciprocal devices.

In the field of magnonics, unidirectionality also plays an important role in view of the possible downscaling device dimensions. A unidirectional SW is essential for building SW insulators and SW diodes, which serve as building blocks for magnonic computing architectures. If the SW transmit is not unidirectional, other effects, such as the energy backflow, may restrict the wide application of SW devices and circuits. A magnetostatic surface SW (MSSW) traveling along the $+y$ axis is localized at the upper surface of a magnetic thin film, while a surface wave traveling along the $-y$ axis is localized at the lower surface of the film. The two SWs have the same frequency and their localization surface can be controlled by the external bias magnetic field [33].

In the presence of an interfacial Dzyaloshinskii–Moriya interaction (iDMI), we deal with frequency asymmetry with two counter-propagating waves with different frequencies. In this paper, we review several recently developed methods for achieving unidirectional SW propagation and devices.

2. Nonreciprocity of MSSWs

2.1. Theoretical background of nonreciprocal surface waves

The propagation of MSSWs is nonreciprocal due to the exponential decay of the SW amplitude from the two surfaces. In the MSSW mode configuration, the magnetization direction is in the film plane and perpendicular to the wavevector direction, as illustrated in figure 1(a). The MSSW is often known as Damon–Eshbach (DE) surface SWs [33] and they could travel from the left to right across the magnetic film while no equivalent waves can travel in the opposite direction [34]. The wavevector of a plane wave is given as $k = \hat{x}k_x + \hat{y}k_y + \hat{z}k_z$. The reflections from the top and bottom surfaces continuously reverse the sign of k_z and a static condition can be fulfilled with the magnetostatic potential in the film as [35]:

$$\Psi = \Psi_0 e^{ikr} \frac{\left(e^{ik_z z} + e^{-ik_z z}\right)}{2} = \Psi_0 \cos\left(k_z z\right) e^{ivk_y y}, \quad (1)$$

where Ψ_0 is the arbitrary amplitude and the parameter $v = \pm 1$ indicates the propagating direction (antiparallel $(+1)$ and parallel (-1) to the y axis). The potential of the modes above and below the film can be assumed as:

$$\Psi_{\text{up}} = C e^{-k_y z + ivk_y y}, \Psi_{\text{down}} = D e^{k_y z + ivk_y y}. \quad (2)$$

The Walker's equation for in the film can be written as

$$(1 + \chi)\left(k_z^2 + k_y^2\right) = 0, \quad (3)$$

which requires $k_z^2 = -k_y^2$. Here, $\chi = \frac{\omega_0 \omega_M}{\omega_0^2 - \omega^2}$, where $\omega_0 = -\gamma\mu_0 H_0$ and $\omega_M = -\gamma\mu_0 M_S$. The SWs propagate in the y direction, so k_y is real and k_z is imaginary. We could replace the potential in the film as:

$$\Psi = (\Psi_{0+} e^{kz} + \Psi_{0-} e^{-kz}) e^{ivky}. \quad (4)$$

To fulfil the boundary conditions at the film surface as well as the normal vector, the condition gives:

$$\begin{bmatrix} (\chi + 2 - v\kappa)e^{kd/2} & -(\chi + v\kappa)e^{-kd/2} \\ -(\chi - v\kappa)e^{-kd/2} & (\chi + 2 + v\kappa)e^{kd/2} \end{bmatrix} \begin{bmatrix} \Psi_{0+} \\ \Psi_{0-} \end{bmatrix} = 0, \quad (5)$$

where $\kappa = \frac{\omega\omega_M}{\omega_0^2 - \omega^2}$ and d is the film thickness. The dispersion relation (frequency vs wavevector) of MSSWs can then be obtained when the determinant of the matrix is vanishing:

$$\omega^2 = \omega_0\left(\omega_0 + \omega_M\right) + \frac{\omega_M^2}{4}\left[1 - e^{-2kd}\right]. \quad (6)$$

The potential function of the MSSW can be expressed as:

$$\Psi = \Psi_0 \left(e^{kz} + \frac{\chi + 2 - v\kappa}{\chi + v\kappa} e^{kd-kz}\right) e^{ivky}. \quad (7)$$

The potential function in the magnetic film decays exponentially along the film thickness direction, as shown in figure 1(a). When changing the propagation direction, the high potential mode shifts from one surface to the other, which is responsible for the SW nonreciprocity. In thick films with $d \gg \lambda$ (λ is the SW wavelength) and $kd \gg 1$, the MSSW only propagates on the top or bottom film surface and unidirectional SWs can be detected either electrically with a microwave antenna patterned on top of the magnetic film [40, 41] or optically by Brillouin light scattering (BLS) spectroscopy [38, 39]. The two MSSWs waves have the same frequency and the propagation direction on the two surfaces is defined by the vectorial product $\vec{k} = \vec{H} \times \hat{n}$, where $\hat{n}$ is the unit vector normal to the film surface. This suggests that by changing the direction of the external magnetic field, the nonreciprocity can be reversed. We investigate the most relevant case for applications: the waves propagating in in-plane magnetized ferromagnetic films at a particular angle to the applied magnetic field. In addition, Kostylev theoretically demonstrated that the fundamental mode of the dipole-exchange spectrum in a thin ferromagnetic metallic film is localized at the film surface opposite the localization surface of the DE surface SWs [42], while such an effect cannot affect the SW nonreciprocity of the SW excitation by microwave antennas.

The localization of the modes on the two surfaces of the film is explained by considering the asymmetry of the dynamic dipolar fields, which create volume and surface magnetic charges which in turn generate dipolar magnetic fields. On the lower surface, the two fields add up while, on the upper one, they partially offset each other. This asymmetry of the dipolar field is at the origin of the localization asymmetry of the mode at the film surfaces. To compensate for this asymmetry, dynamic magnetization increases its amplitude by precession near the surface of the film, where the dynamic dipolar field is smaller [43].
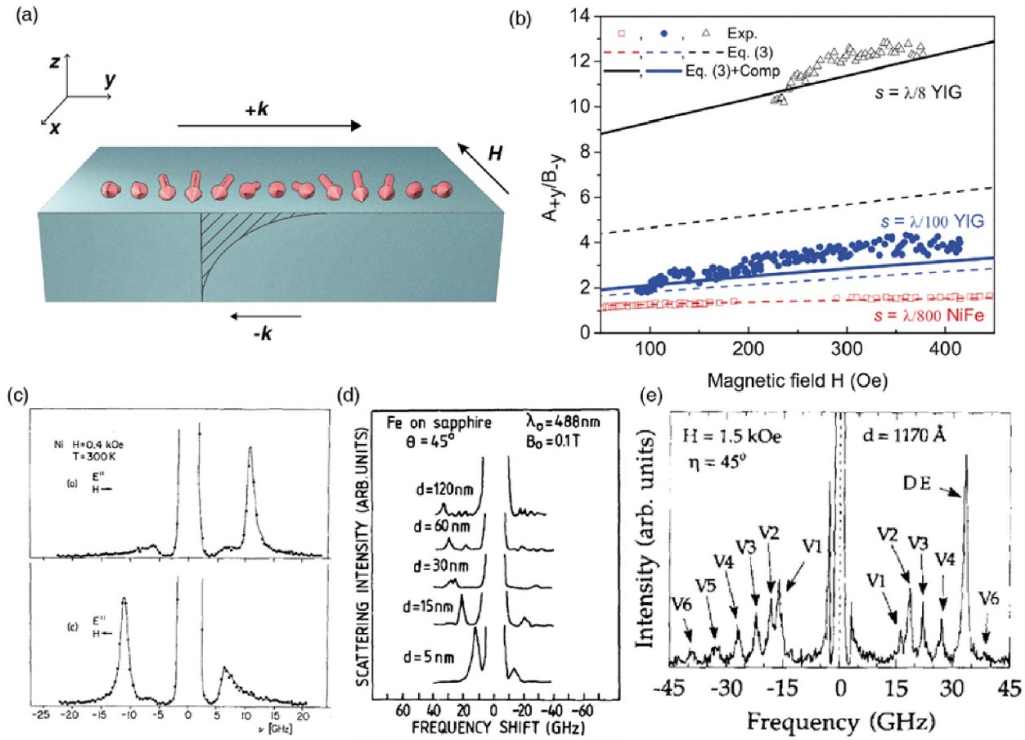
Figure 1. (a) An illustration of nonreciprocal DE-mode SWs propagating on the opposite film surfaces along the *y*-direction. The external magnetic field is applied perpendicular to the SW wavevector. (b) Nonreciprocity ratios of magnetic films with different thicknesses. The experimental and theoretical calculated results of a 20 nm permalloy film, a 160 nm YIG film and a 2 μm YIG film are presented. Reprinted from [36], with the permission of AIP Publishing. (c) BLS spectra of Ni film with the thickness of 50 μm. One can see how reversal of the magnetic field direction changes the peak position from the Stokes to anti-Stokes side of the spectra. Reprinted from [37], with the permission of AIP Publishing. (d) BLS spectra of Fe films on sapphire substrates with different thicknesses in the range from 5 to 120 nm. For thickness larger than 15 nm PSSWs resonating across the thickness of the magnetic film are also visible. Reprinted from [38], with the permission of AIP Publishing. (e) A BLS spectrum of a Fe/GaAs (100) sample of thickness 1170 Å shows the presence of several well-resolved and sharp peaks. The first six peaks associated with the PSSWs (Vl–V6) and the surface SW mode (DE), observed only in the anti-Stokes side of the spectrum, have been labelled. Reprinted from [39]. Copyright (1995), with permission from Elsevier.

2.2. Unidirectional SWs in thick magnetic films

Unidirectional MSSWs were detected in thick magnetic films by microwave-based technology for several decades in thick Yittrium Iron Garnet (YIG) slabs [40, 41]. In 2014, Wong *et al* experimentally obtained the SW amplitude ratios by measuring SWs propagating in opposite directions in magnetic films with different thicknesses, including a 20 nm permalloy film, a 160 nm YIG film and a 2 μm YIG film [36]. Two microwave antennas are fabricated on the top surface of the film with a separation distance of 8 μm. By directly comparing the SW amplitude extracted by scattering parameters, S_{12} and S_{21}, from a vector network analyzer, the SW nonreciprocity is found to increase with an increasing sample thickness, as shown in figure 1(b). However, when the thickness of the YIG film is 254 μm, the nonreciprocity is greatly enhanced and SW unidirectionality is achieved. In 2009, Demidov *et al* found that, using a stripe antenna, the excitation of the MSSWs is nonreciprocal in amplitude, although the decay rate of the left and right of the antenna is the same [44]. In addition, it is found that when using a low-damping thick YIG film, the unidirectional SWs can convey heat and, at the sample, end up to 10 mm from the microwave source [45].

Madami *et al* [46] studied the focusing of magnetostatic backward volume waves (MSBVWs) excited by a curvilinear microwave coplanar waveguide in 5 mm-thick epitaxial YIG film within an in-plane bias field oriented along the symmetry axis of the transducer. It was shown by both the micro-BLS technique and micromagnetic simulation that two-dimensional maps of MSBVW beam intensity at distances larger than the focus position demonstrate nonreciprocity and absence of mirror symmetry with respect to the direction of the bias field. These effects result from the nonreciprocity of MSBVWs traveling at an angle to the bias field direction.

The unidirectional SW propagation in magnetic thin films is challenging to achieve in thin magnetic films, so engineering the nonreciprocity of MSSWs is very important. In 2016, Kwon *et al* found a way to enhance the nonreciprocity by putting a Ta layer on top of permalloy [47]. They found that the nonreciprocity depends on the Ta thickness, which induces a modification of the interfacial anisotropy. The nonreciprocity ratio was found to reach a value of 60 in the time and frequency domain.

The mode localization of MSSWs can also be detected by BLS spectroscopy, which is an optical technique based on the inelastic scattering of photons with thermal magnons [48, 49].

J. Phys. D: Appl. Phys. **55** (2022) 123001

Topical Review

Sandercock *et al* studied surface magnons in thick Fe and Ni films and, by reversing the direction of the bias magnetic field, observed that the sharp peak associated with the DE wave moves from one side of the spectrum to the other, as the signature of the SW nonreciprocity, as shown in figure 1(c) [37]. Grünberg *et al* studied perpendicular standing SWs (PSSWs) and the DE surface wave in Fe films by BLS and found that the remarkable Stokes-anti-Stokes intensity asymmetry indicated the SW nonreciprocity [38]. For magnetic films thinner than the penetration depth of light in metallic films (typically of 15–20 nm), the DE mode can be detected on both the Stokes and anti-Stokes side of the BLS spectra while, for larger film thickness, it is observed on one side only. In a 1170 Å thick Fe film, Hicken *et al* found that the surface SW mode exhibited strong nonreciprocity, being observed on one anti-Stokes side of the spectrum, while the PSSW modes were reciprocal, as shown in figure 1(e) [39].

Modification of the MSSW dispersion (frequency vs wavevector) to achieve unidirectional SW propagation can also be achieved in exchange and dipolar-coupled ferromagnetic films. Grassi *et al* [50] showed careful engineering of the dispersion for MSSWs in a CoFeB/NiFe bilayer, where it is possible to reduce the group velocity of waves traveling in a particular direction to a very low value (slow waves) while maintaining a large value for those propagating the other way. Similar results were obtained by Mruczkiewicz *et al* [51] in a NiFe/Ni bilayer.

Gallardo *et al* [52] demonstrated that the dipolar interaction produced by the dynamic magnetizations between two ferromagnetic layers separated by a nonmagnetic spacer is a notable source of nonreciprocity in the SW frequency, with a remarkable property of reconfigurability that relies on control of the relative magnetic orientation of the interacting ferromagnetic layers.

3. Unidirectional SWs in ferromagnetic films with DMI

3.1. Theory of spin-wave dispersion in the presence of iDMI

The DMI is the asymmetric exchange interaction in magnetic systems, which could induce chiral magnetic textures such as skyrmions and chiral domain walls. The DMI between two neighbouring spins takes the form [53]:

$$H_{DMI} = -\boldsymbol{D}_{12} \cdot (\boldsymbol{S}_1 \times \boldsymbol{S}_2), \tag{8}$$

where $\boldsymbol{S}_1$ and $\boldsymbol{S}_2$ are neighbouring spins and $\boldsymbol{D}_{12}$ is the DM vector. Two types of DMI can be classified depending on the type of inversion symmetry breaking. The iDMI corresponds to the inversion symmetry breaking at the interface, which is inversely proportional to the film thickness. Typical magnetic systems which host iDMI are magnetic multilayers, where one layer should provide strong spin–orbit couplings, such as Pt, Ta, W and Ir. The bulk DMI is found mostly in B20 structures such as MnSi and FeGe. In this section, we mainly focus on the iDMI.

When SWs propagate in a magnetic system with iDMI, the dispersion is reformed due to the inversion symmetry breaking. Consider that SWs propagate in the film plane and are perpendicular to the external magnetic field in a magnetic film with iDMI, as shown in figure 2(a). The SW dynamics can be described by the Landau–Lifshitz–Gilbert (LLG) equation as:

$$\frac{d\widehat{\boldsymbol{m}}}{dt} = -\gamma\mu_0\widehat{\boldsymbol{m}} \times \boldsymbol{H}_{eff} + \alpha\left(\widehat{\boldsymbol{m}} \times \frac{d\widehat{\boldsymbol{m}}}{dt}\right), \tag{9}$$

where α is the damping parameter. The effective field $\boldsymbol{H}_{eff}$ can be written as:

$$\boldsymbol{H}_{eff} = vH\boldsymbol{x} + \frac{2A}{\mu_0 M_S}\nabla^2\widehat{\boldsymbol{m}} - \frac{2D}{\mu_0 M_S}\left(\boldsymbol{x} \times \frac{d\widehat{\boldsymbol{m}}}{dt}\right) + \boldsymbol{H}_{dip}, \tag{10}$$

where H is the external field, $v = \pm 1$ indicates the propagating direction, A is the exchange stiffness, D is the iDMI constant and $\boldsymbol{H}_{dip}$ is the dipolar field depending on the film thickness and the wavevector. The dispersion, by neglecting the nonlocal magnetostatic contribution, can be expressed as:

$$\omega = \gamma\mu_0\left[\left(H + \frac{2A}{\mu_0 M_S}k^2\right)\left(H + M_S + \frac{2A}{\mu_0 M_S}k^2\right)\right]^{\frac{1}{2}} + \frac{2vD}{\mu_0 M_S}k. \tag{11}$$

In the small k limit, where the exchange interaction can be neglected, the dispersion is reformed as:

$$\omega = \gamma\mu_0[H(H + M_S)]^{\frac{1}{2}} + \frac{M_S^2|k|d}{4[H(H + M_S)]^{\frac{1}{2}}} + \frac{2vD}{\mu_0 M_S}k. \tag{12}$$

The dispersion of SWs is then asymmetric, depending on the propagation direction, and shows a linear dependence of the k when considering the iDMI. The calculated SW dispersion with $D = -1.5, 0, 1.5$ mJ m^{-2} in the large k limit is shown in figure 1(b), where the saturation magnetization $M_S = 800$ kA m^{-1}, the exchange constant $A = 1.3 \times 10^{-11}$ J m^{-1} and the thickness $d = 1$ nm is used in the calculation.

3.2. Nonreciprocal and unidirectional SW propagation with DMI

The asymmetric dispersion induced by iDMI results in the nonreciprocal SWs in the frequency domain. BLS is an efficient method to detect the asymmetric SW dispersion with the wavevector resolution [57–59]. The propagating SWs with opposite directions give rise to the Stokes and anti-Stokes peaks, which can characterize frequency differences induced by the asymmetric dispersion. In 2015, Di *et al* directly observe the iDMI in a Pt/Co/Ni multilayer by BLS [60]. An iDMI constant of 0.44 mJ m^{-2} is found and the linewidths of the counter-propagating SWs are different, which is in agreement with the theoretical simulations. Tacchi *et al* further investigate the effect of the heavy metal thickness of the iDMI in Pt/CoFeB films by BLS [54]. The authors found that by
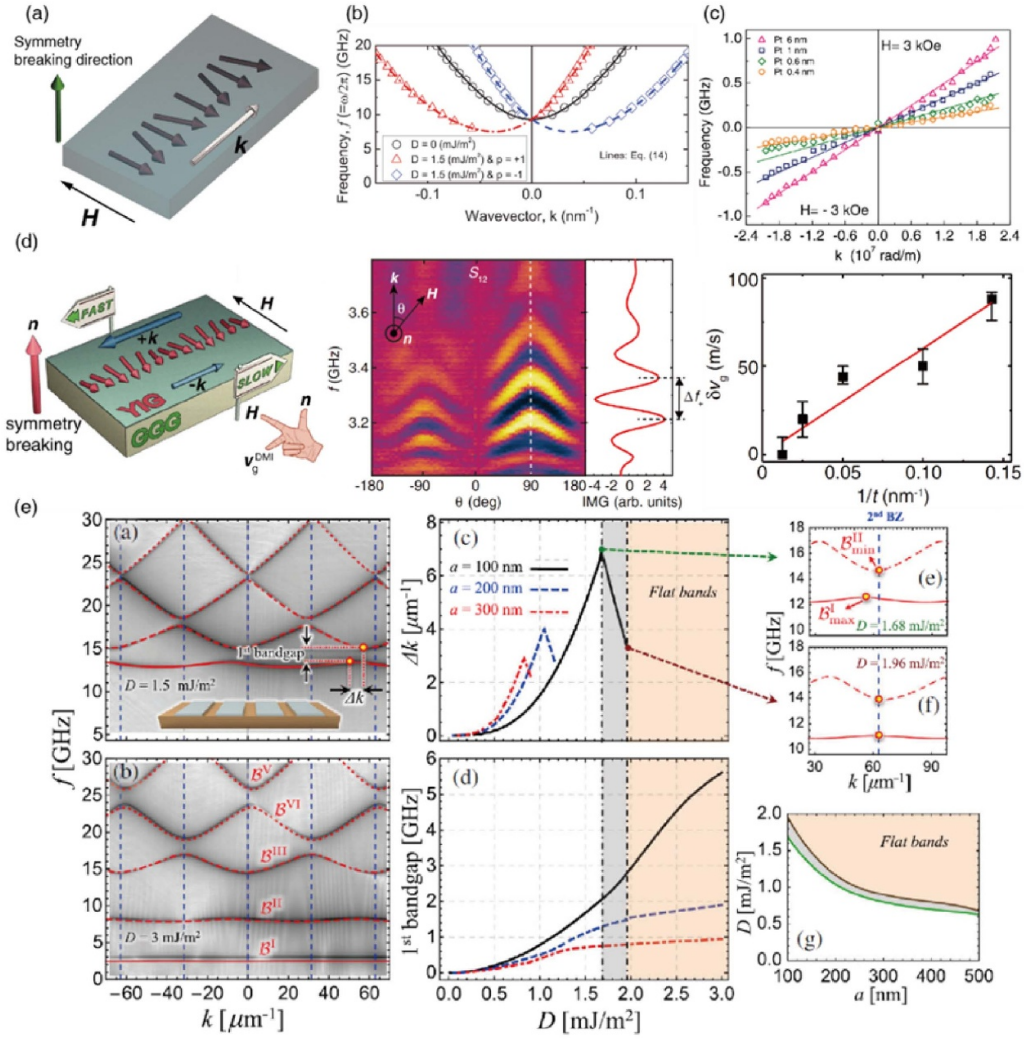
Figure 2. (a) Geometry of a magnetic film with iDMI. (b) Asymmetric SW dispersion induced by iDMI with large wavevectors. Reprinted (figure) with permission from [53]. Copyright (2013), the American Physical Society. (c) Wavevector dependence of frequency difference between Stokes and anti-Stokes modes in Pt/CoFeB films by varying the Pt thickness. Reprinted (figure) with permission from [54]. Copyright (2017), the American Physical Society. (d) Chiral SW group velocities in a YIG thin film with iDMI. Reprinted (figure) with permission from [55]. Copyright (2020), the American Physical Society. (e) Flat bands observed in magnonic crystals with periodic iDMI. Reprinted (figure) with permission from [56]. Copyright (2019), the American Physical Society.

increasing the Pt thickness, the iDMI increases and saturates to a value around 0.45 mJ m^{-2} for Pt thicknesses larger than 2 nm, as shown in figure 2(c).

IDMI and nonreciprocal SWs can also be detected and a chiral SW group velocity is found to be induced by iDMI in ultrathin magnetic garnet films, where SWs propagating in the chirally favoured direction travel faster than in the counter-direction, as shown in figure 2(d) [55, 61]. The chirality beha-viour of SW group velocities is attributed to a DMI-induced drift group velocity whose direction follows a right-handed rule as:

$$v_{\mathrm{DMI}} = \left[\left(\widehat{\mathbf{n}} \times \widehat{\mathbf{H}} \right) \cdot \widehat{\mathbf{k}} \right] \frac{2\gamma}{M_{\mathrm{S}}} D. \tag{13}$$

The orientation of the drift velocity can be controlled by the external magnetic field as well as the propaga-tion direction. In the spectra extracted from the electrical

propagating SW spectroscopy, the SW group velocity can be calculated as:

$$v_{\mathrm{g}} = \frac{\mathrm{d}\omega}{\mathrm{d}k} = \Delta f \cdot s, \tag{14}$$

where Δf is the frequency span indicating an SW phase change of 2π, and s is the SW propagation distance. One can observe in figure 2(d) that by reversing either the SW propagation dir-ection or the external magnetic field, the SW velocity shifts due to the iDMI-induced drift velocity. The asymmetry of SW group velocity increases when decreasing the film thickness, indicating that the DMI is an interfacial effect in thin YIG films. An overview of the experimental techniques as well as their theoretical background and models for the quantification of the DMI constant D on iDMI measurements can also be found in [62].

Taking advantage of the asymmetric SW dispersion induced by the iDMI, the lowest frequency point in the SW

J. Phys. D: Appl. Phys. **55** (2022) 123001

Topical Review

dispersion shifts from $k = 0$. Ma *et al* [63] found that when the excitation frequency is below the frequency of the mode with $k = 0$, SWs can only propagate in one direction. By using micromagnetic simulations, the authors present spatial maps of SWs with different frequencies. Due to different velocities and relaxation times, SWs with a frequency higher than Ferromagnetic Resonance (FMR) also propagate nonreciprocally in opposite directions with different decay lengths. Although unidirectional SWs are found in magnetic multilayers with iDMI, the experimental realization of the unidirectional SW propagation in such systems is still missing. Finding a magnetic thin film with both large iDMI and low damping is required for functional unidirectional SWbased devices.

3.3. Periodic DMI-based magnonic crystals with asymmetric band structures

Magnonic crystals (MCs) are periodic magnetic structures that can modify the band structure of SWs in GHz frequencies [64–70]. The asymmetric dispersion induced by iDMI could host nonreciprocal SW propagation. Gallardo *et al* investigated periodic iDMI-based magnonic crystals [56] using theoretical calculations and micromagnetic simulations. The periodic iDMI can be realized by patterning periodic heavy metal wires with strong spin–orbit coupling on top of a ferromagnetic thin film. Theoretical as well as numerical calculations are performed and the simulated magnon band structures are shown in figure 2(e). Due to the periodic iDMI, the SW dispersion is nonreciprocal and the magnonic band gap opens. By increasing the iDMI value, the bottom magnon bands of the dispersion shifts down and the first band gap is enhanced. The indirect band gaps are observed due to the fact that the maximum of the first band and the minimum of the second band shift in a different way when changing the iDMI value.

As the maximum of the first band reaches the second Brillouin zone, this branch becomes flat when the iDMI value is large. The larger periodicity favours the flat bands due to the reduction of the interlayer coupling of SWs underneath heavy metal wires. Below the heavy metal wires, the nonreciprocal SWs are also found to propagate, due to the non-zero phase velocities in the regions where the iDMI is non-zero.

Recently, Silvani *et al* [71] also presented the impact of the iDMI on the band structure of a one-dimensional magnonic crystal using micromagnetic simulations. The authors found flat bands at positive wavevectors when a large iDMI strength exists. Those flat modes are separated by forbidden gaps whose amplitudes depend on the value of *D*. By performing the time evaluation of the magnetization dynamics of the flat modes, the authors found that these modes are confined in specific regions and propagate only along the positive *x*-direction, indicating the SW unidirectionality. The formation of the indirect band gap as well as the low-frequency flat bands are demonstrated in the system of the magnonic crystal with periodic DMI, which encourages further studies in the investigation of chiral magnonic crystals and other related physical properties.

Asymmetric band structure has also been predicted and observed in magnonic crystals without iDMI. Mruczkiewicz *et al* theoretically investigated the impact of a perfect metal overlayer on the SW dispersion relation of 1D bi-component MCs [72] and in thin NiFe film dynamically coupled to an array of Ni stripes [51]. In both cases, the nonreciprocity is manifested in the shifting of the magnonic bandgap edges from the Brillouin zone border.

4. Unidirectional emission of SWs by arrays of nanomagnets

4.1. Theoretical analysis of chiral pumping of SWs with local magnetic transducers

By placing an array of nanomagnets on top of a low damping magnetic insulator thin film, unidirectional SWs can be generated by the dynamics of the nanomagnets due to the chiral spin pumping effect [73]. Since the magnetic film is ultrathin (with a thickness of tens of nanometres), the DE-mode-induced SW nonreciprocity can be neglected. Typical heterostructures, where magnetic nanowires (Co) are placed on top of the low-damping magnetic thin film (YIG), are investigated, as shown in figure 3(a) [73]. Assuming the magnetic thin film has polycrystalline structures with isotropic in-plane magnetic properties and ignoring the PSSWs, the hybrid system can be treated as quasi-one-dimensional and the Hamiltonian can be written as [73]:

$$\frac{\widehat{\mathcal{H}}}{\hbar} = \sum_n (\omega_n^+ \hat{\beta}_{+k} \hat{\alpha}^\dagger + \omega_n^- \hat{\beta}_{-k} \hat{\alpha}^\dagger), \qquad (15)$$

where $\hat{\alpha}^\dagger$ is the creative operator of the magnon modes in the magnetic nanowires, and $\hat{\beta}_{+k}$ and $\hat{\beta}_{-k}$ are creative operators of propagating SWs in the magnetic film with opposite directions. The coupling strengths between magnon modes are:

$$\omega_n^+ = -\frac{2\gamma}{n\pi} \sigma_n \sqrt{(\mu_0 M_S^W)(\mu_0 M_S^F)} \int \widehat{m}_W^* \widetilde{\Lambda}^* \widehat{m}_F e^{kx} dx$$

$$\omega_n^- = -\frac{2\gamma}{n\pi} \sigma_n \sqrt{(\mu_0 M_S^W)(\mu_0 M_S^F)} \int \widehat{m}_W^* \widetilde{\Lambda} \widehat{m}_F e^{kx} dx \quad (16)$$

with the SW wavenumbers $k = \pi n/a$ with $n = 2, 4, 6 \dots$ propagating along the $+\boldsymbol{y}$ direction for ω_n^+ and the $-\boldsymbol{y}$ direction for ω_n^- and $\sigma_n = \sin\left(\frac{kw}{2}\right)\left(1 - e^{-kh}\right)$. $\mu_{S0} M_S^W$ and $\mu_0 M_S^F$ are the saturation magnetization of magnetic nanowires and film, respectively. Here, $\widehat{m}_W = (\hat{m}_x, \hat{m}_y)$ describes the magnetization dynamics in nanowires and $\hat{m}_x = \left(\frac{a}{4hw}\sqrt{\frac{H_0 + M_S^W N_{yy}}{H_0 + M_S^W N_{xx}}}\right)^{1/2}$ and $\hat{m}_y = \left(\frac{a}{4hw}\sqrt{\frac{H_0 + M_S^W N_{xx}}{H_0 + M_S^W N_{yy}}}\right)^{1/2}$, where N_{xx} and N_{yy} are demagnetization factors; $\widetilde{\Lambda} = \begin{pmatrix} 1 & i \\ i & -1 \end{pmatrix}$ and $\widehat{\boldsymbol{m}}_F = (\hat{m}_x^k, \hat{m}_y^k)$ describes the magnetization dynamics in the magnetic film and $i\hat{m}_x^k = \hat{m}_y^k = i\left(\frac{1}{4t}\right)^{1/2}$. When $|\omega_n^+| \neq |\omega_n^-|$, the interlayer dipolar coupling is chiral and the
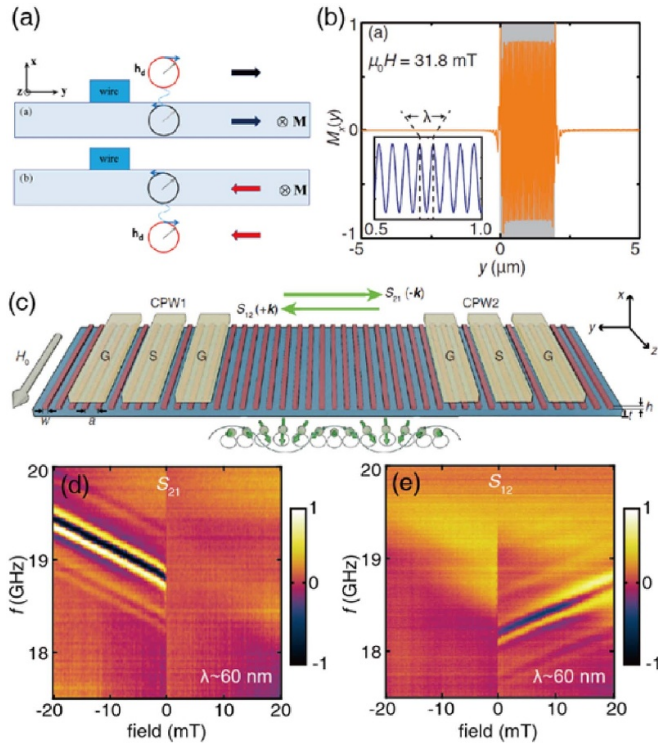
Figure 3. (a) An illustration of unidirectional SWs emitted by nanomagnets. Reprinted (figure) with permission from [73]. Copyright (2019), the American Physical Society. (b) Theoretical calculation of the magnon trap with two magnetic nanowires. Reproduced from [74]. (c) A sketch of propagating SWs in a low-damping YIG film with a Co nanowire array patterned on top. Reprinted (figure) with permission from [75]. Copyright (2019), the American Physical Society. (d), (e) Microwave transmission spectra, S_{21} and S_{12}, of unidirectional SWs with the wavelength of 60 nm.

chirality ratio of the counter-propagating SWs can be defined as:

$$\eta = \left| \frac{\left(\frac{\omega_n^+}{\omega_n^-}\right)^2 - 1}{\left(\frac{\omega_n^+}{\omega_n^-}\right)^2 + 1} \right|. \tag{17}$$

In the parallel state, where the magnetization in nanowires is parallel to that of the film, $\omega_n^- = 0$ $\omega_n^+ \neq 0$ and the SWs only propagate in one direction. In the antiparallel state, $\widehat{\boldsymbol{m}}_{\mathrm{F}} = \left(\hat{m}_x^k, -\hat{m}_y^k\right)$ and $\omega_n^+ = 0$ $\omega_n^- \neq 0$. The chirality of SWs is reversed and SWs only propagate in the opposite directions. In addition, the unidirectional SWs emitted by a nanomagnet are found to be perfectly trapped by a second initially passive magnet by a dynamical interference effect, as shown in figure 3(b) [74]. Moreover, due to the chiral spin pumping effect, the line width broadening in a magnetic heterostructure consisting of a Co nanowire grating dipolar-coupled to a YIG film is probed by BLS microscopy, indicating tunable magnetic damping [76]. Unidirectional SWs are found in this system and oscillating behaviour of the magnon population in Co nanowire grating is observed due to the magnon trap effect.

4.2. Unidirectional exchange SWs emitted by a nanoscale magnetic grating

An experimental investigation is also conducted using a nanoscale magnetic array to excite unidirectional SWs [75, 77]. A Co nanowire array is patterned on top of an ultra-low-damping YIG thin film with a period of 600 nm. On top of the nanowire array, two identical coplanar waveguides (CPW) are fabricated to excite and detect propagating SWs. Due to the large demagnetization field, the magnetization of Co nanowires cannot be switched when the field is swept from positive to negative values, forming the parallel and antiparallel states, respectively. Due to the magnon–magnon coupling effect [78–82], the high-order exchange SWs with the wavelength of 60 nm can be excited and figures 3(d) and (e) show the transmission spectra S_{21} and S_{12}, respectively. Unidirectional SWs can be observed and, by switching the parallel and antiparallel states, the propagation SW direction is reversed, which is in line with the theoretical calculations.

Since the demagnetization field in YIG film is very small, we could rotate the external field angle to change the angle between the magnetization of the nanowires and YIG film. When the external field is tilted away from the parallel direction to the nanowire, the chirality is broken and the SWs are not unidirectionally propagating anymore. We find that at the angle around 60°, the SW nonreciprocity is totally suppressed. The material engineering of such devices could further enhance device functionalities. It is promising to use antiferromagnetic materials for exciting, even shorter wavelength unidirectional SWs due to the sub-THz resonance frequencies.

5. Unidirectional SWs in spin textures

5.1. Nonreciprocal and unidirectional SW propagation along spin textures

Spin textures are non-collinear magnetic orders in the magnetic ground state, which are due to the interplay between dipolar interaction, symmetric Heisenberg exchange interaction and DMI [83–97]. By combining with spin textures such as domain walls, vortices and skyrmions, multiple functionalities can be realized in SW-based devices. Magnetic domain walls are boundaries between different magnetic domains and SWs can be channelled inside the domain wall. In 2015, Garcia-Sanchez *et al* demonstrated that SWs can propagate in narrow magnonic waveguides based on domain walls [98]. They found that SWs can travel in both Bloch- and Néel-type domain walls. In Néel-type domain walls, SWs are strongly nonreciprocal due to the iDMI. In 2016, Wagner *et al* experimentally demonstrated that magnetic domain walls can serve as a reconfigurable SW nanochannel [99]. SWs propagating inside magnetic-vortex-stabilized domain walls are also imaged using BLS and scanning transmission x-ray microscopy (STXM), respectively [100, 101].

Unidirectional SWs can also propagate in a Bloch-type domain wall (see figure 4(a)), which has recently been demonstrated by Henry *et al* [102]. In an array of parallel domain walls in the stripe domain configuration, SW dispersion is
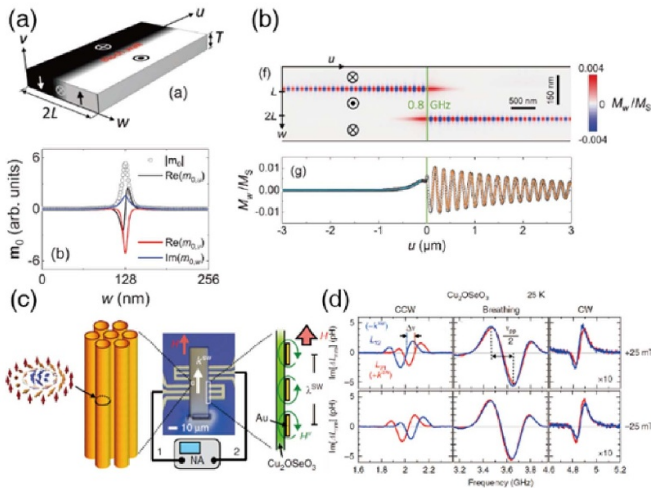
J. Phys. D: Appl. Phys. **55** (2022) 123001

Topical Review

Figure 4. (a) A sketch of a magnetic domain wall separating neighbouring perpendicularly magnetized domain walls. Reprinted (figure) with permission from [102]. Copyright (2019), the American Physical Society. (b) Unidirectional propagating of SWs inside the neighbouring Bloch-type domain walls. Reprinted (figure) with permission from [102]. Copyright (2019), the American Physical Society. (c) Magnetic skyrmion strings in a Cu_2OSeO_3 lamella placed on top of two CPWs. Reproduced from [104]. CC BY 4.0. (d) Microwave transmission spectra of propagating SWs along skyrmion strings in counterclockwise (CCW), breathing and clockwise (CW) states. Reproduced from [104]. CC BY 4.0.

modified due to the sequence of up/down domain walls with opposite nonreciprocity. If SWs are excited within the gap formed between two domain wall channelled branches in its dispersion, unidirectional SWs can be launched, as shown in figure 4(b). Furthermore, if a nanomagnet array is placed on top of a Néel-type domain wall, unidirectional SWs can also be emitted due to the chiral spin pumping effect [103].

The interplay between SWs and skyrmions has attracted considerable attention recently. When extended to a three-dimensional system, a skyrmion can form a string-like structure consisting of stacks of two-dimensional skyrmions, as shown in figure 4(c) [104]. Materials like Cu_2OSeO_3 can host those skyrmion strings in cryogenic temperatures [105]. Using all-electrical SW characterizations, Seki *et al* investigated the propagating SWs inside skyrmion strings in Cu_2OSeO_3 lamellas [104]. The authors find that the propagating SWs are reciprocal in frequencies and decay lengths as well as group velocities, which strongly depend on the excitation modes, namely, clockwise, counter-clockwise and breathing modes, as shown in figure 4(d). The nonreciprocal SWs in skyrmion strings show properties for unidirectional information transfer in a topological object. Theoretical studies have also demonstrated the elementary process for the skyrmion motion driven by SWs [106]. It is found that propagating SWs can be scattered by the skyrmion by solving the LLG equation, which is determined by the skyrmion Hall angle. The Gilbert damping as well as the SW amplitude could influence the speed of the skyrmion motion. Due to topological protection, the skyrmion cannot easily be deteriorated by SWs. Beyond magnetic domain walls and skyrmions, the investigation of unidirectional SWs in

other magnetic textures, such as vortices and helimagnetic spirals, is required.

5.2. Unidirectional SWs excited by spin texture-based magnonic nanoantennas

Magnetic textures can also be used to excite SWs with their high-frequency dynamic properties. In 2016, Van de Wiele *et al* proposed a method using pinned magnetic domain walls to excite SWs with short-wavelengths [107]. Then, Holländer *et al* demonstrated that magnetic domain walls can be an effective antenna for generating broadband SWs [108]. In 2020, Albisetti *et al* found that by using patterned shaped micro-antennas such as domain walls in synthetic antiferromagnetic thin films, spatially shaped SW wavefronts can be fully controlled, as shown in figure 5(a) [109]. By sweeping a heated scanning probe, the exchange bias direction can be modified as well as the underlayer CoFeB magnetization, and domain walls can be patterned in a reconfigurable manner [110]. Using STXM, the focusing of SWs emitted by a curved domain wall can be imaged, as shown in figure 5(b). The spatial profile extracted at the focal point shows the full width at half maximum of the beam amplitude is around 340 nm. This type of curved domain walls emitting SWs shows a strong non-reciprocity due to the particular spin textures.

SWs can also be emitted by magnetic skyrmions. In 2020, Díaz *et al* found that skyrmion–antiskyrmion bilayers can form topological charge dipoles and can efficiently emit SWs with the wavelength down to 100 nm, as shown in figure 5(c) [111]. The different SW patterns are found to depend on the spiral or antispiral spatial profiles. Recently, Chen *et al* proved that chiral SWs can be generated by a magnetic skyrmion on top of a low-damping magnetic thin film, as shown in figure 5(d) [112]. The chirality of the SWs results from the dynamical dipolar coupling between the magnetic bilayer and is determined by the magnetization directions of the magnetic film as well as the film normal direction. Unidirectional SW propagation is observed in a certain direction.

6. Magnonic devices based on unidirectional SWs

6.1. SW diodes and circulators

Unidirectional information transfer is a basic element for modern logic architectures. A diode is a two-terminal electronic device that conducts an electrical current in one direction. The excitation and propagation of unidirectional SWs could result in a crucial functionality in magnonic logic and computing devices, for the ability to build SW diodes, SW insulators, SW interferometers, etc. An SW diode can be designed in imitation of manganic electronic diodes. In 2015, Lan *et al* proposed a method for a reconfigurable SW diode based on chiral bound states in magnetic domain walls with iDMI [113]. In a magnetic film with a Bloch-type domain wall separating neighbouring domains, the bound SWs can propagate identically in both directions in the domain wall without iDMI. However, in the presence of iDMI, SWs propagating in opposite directions
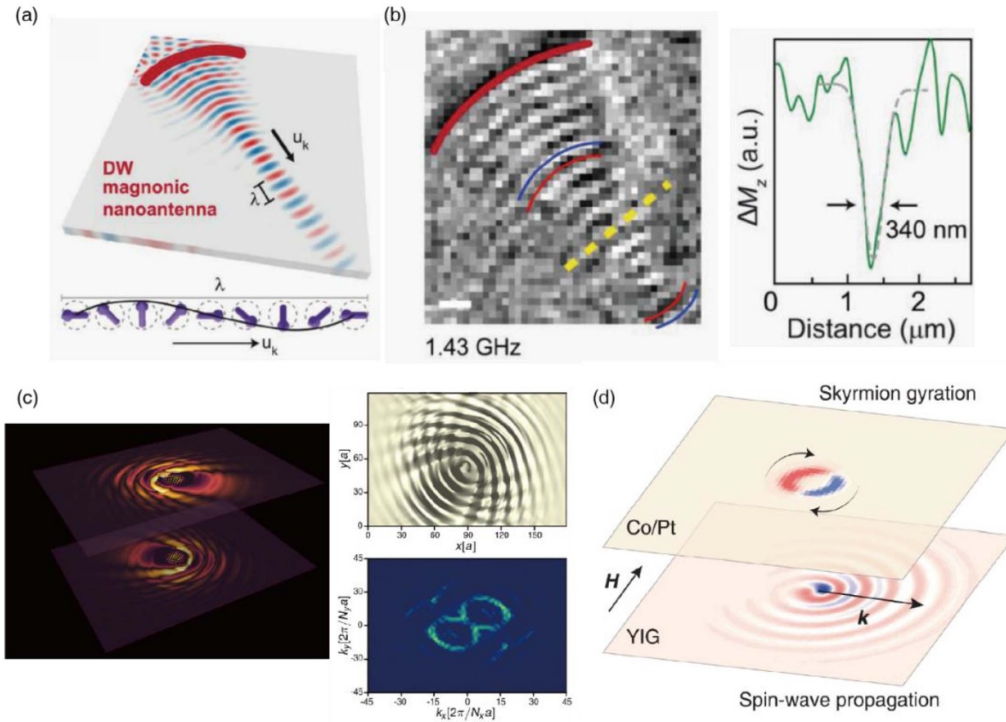
J. Phys. D: Appl. Phys. **55** (2022) 123001

Topical Review

Figure 5. (a) An illustration of a domain-wall-based magnonic nanoantenna. [109] John Wiley & Sons. (Copyright © 2020 WILEY-VCH Verlag GmbH & Co. KGaA, Weinheim.) (b) An STXM image of SWs emitted by a thermal probe patterned domain wall in a ferromagnetic–antiferromagnetic heterostructure. The line plot indicates the width of the SW packet marked as a yellow dotted line in the STXM image. [109] John Wiley & Sons. (Copyright © 2020 WILEY-VCH Verlag GmbH & Co. KGaA, Weinheim.) (c) Skyrmion–antiskyrmion bilayers form a topological charge dipole for exciting SWs with the wavelength down to 100 nm. Reproduced from [111]. (d) A sketch of the chiral emission of exchange SWs in a low-damping YIG film with a skyrmion. Reprinted with permission from [112]. Copyright (2021), the American Chemical Society.
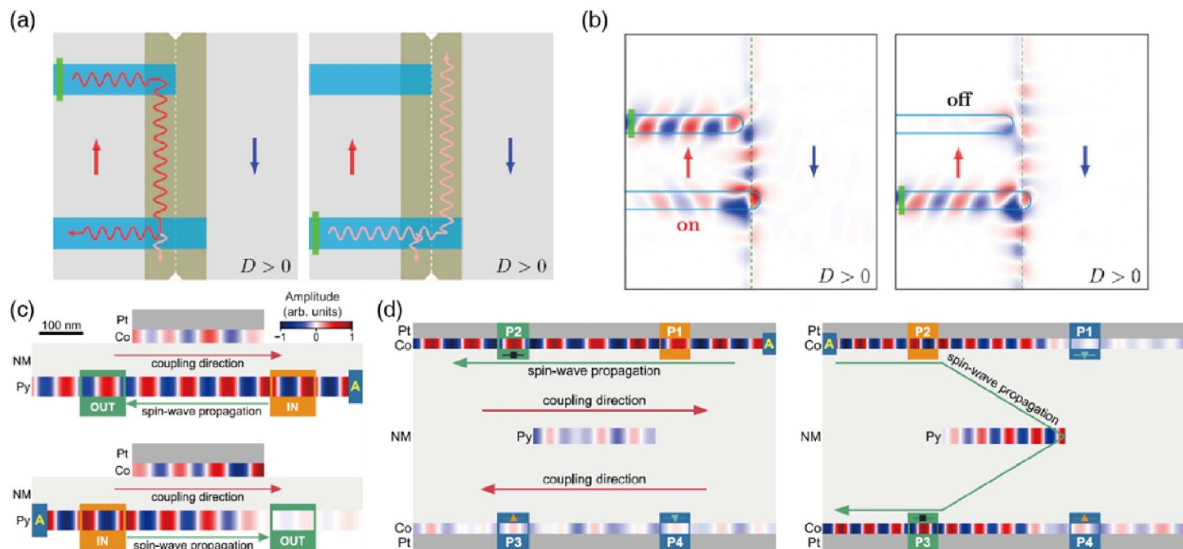

Figure 6. (a) A conceptual illustration of an SW diode based on magnetic domain walls with iDMI. When SWs propagate from the bottom to the top, they can pass by travelling in the left part to the domain wall. SWs cannot pass in the reversed process. Reproduced from [113]. CC BY 3.0. (b) Micromagnetic simulations of the SW diode. Reproduced from [113]. CC BY 3.0. (c), (d) An SW diode and circulator designs based on the unidirectional magnetostatic coupling with iDMI in vertical structures. Reprinted (figure) with permission from [114]. Copyright (2020), the American Physical Society.

are spatially separated to different edges of the domain wall. If two-terminal conduits are placed at the left of the domain wall, a prototypical function of the SW diode can be realized, as shown in figure 6(a). If SWs are excited from the top terminal, they can pass the left part of the domain wall and reach the bottom terminal, while the opposite direction is forbidden due
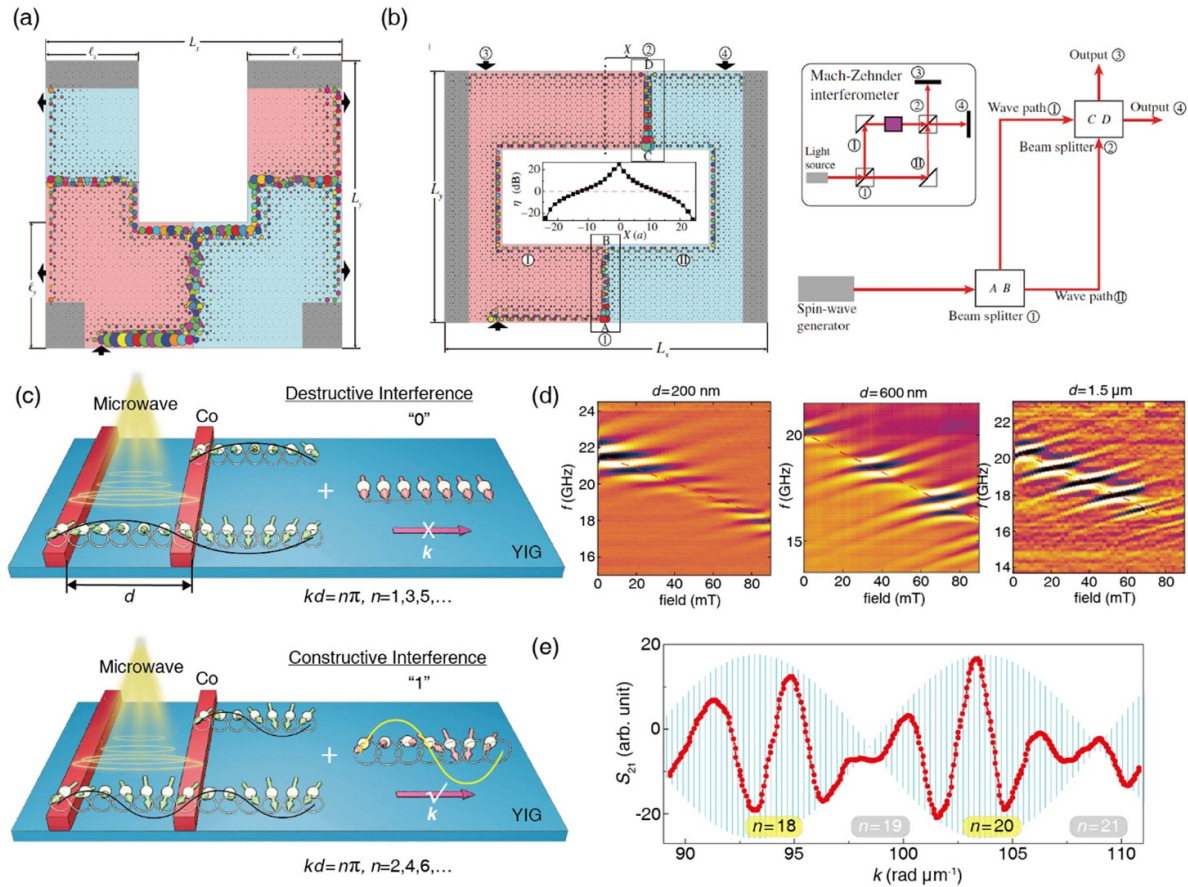
Figure 7. (a), (b) An SW beam splitter and interferometer based on topological chiral edge SWs. Reprinted (figure) with permission from [116]. Copyright (2018), the American Physical Society. (c) A sketch of a nanoscale SW interferometer with two Co nanowires on top of a YIG thin film. Reprinted with permission from [117]. Copyright (2021), the American Chemical Society. (d) SW interference patterns in the frequency domain with varying d and k. Reprinted with permission from [117]. Copyright (2021), the American Chemical Society.

to the fact that SWs can only propagate through the right part of the domain wall. Figure 6(b) shows the micromagnetic simulation results of the SW diode in the forward and reverse directions.

The concept of an SW diode based on the chiral dipolar coupling in two exchange-coupled ferromagnetic layers was proposed by Grassi *et al* [50] They showed that the diode had a wide operation frequency window in the GHz range that can be adjusted by tuning the amplitude of the applied magnetic field, and its forward and reverse directions can be interchanged by switching the polarity of the field.

By using unidirectional magnetostatic coupling induced by the iDMI, SW diodes and circulators can also be designed in a magnetic multilayer system [114]. The concept of the SW diode is shown in figure 6(c). A Py (3 nm)/NM (5 nm)/Co (2 nm)/Pt multilayer is investigated and, due to the unidirectional coupling direction, propagating SWs can only transport in a single direction in Py thin film. A circulator design is also proposed in a similar multilayer structure, as shown in figure 6(d). SWs in Co film can only propagate from port 1 to port 2 due to the weak coupling with the Py. However, if SWs travel from port 2 to port 3, the coupling with Py is strong and the energy can only be transferred between two Co layers. The SW diode and circulator show promising potential as

logic elements in energy-efficient magnonic circuits. The unidirectional SW diodes discussed above are mostly investigated using theoretical calculations and numerical simulations. Practical unidirectional SW diodes with more functionalities and sizes in the submicrometric range are required to build magnonic computing elements and circuits.

6.2. SW interferometers and beam splitters

Topologically protected chiral edge SW modes have been predicted in both magnonic crystals and two-dimensional honeycomb lattices [115, 116]. These SWs are topologically nontrivial and propagate in a unidirectional manner without backward scattering. Using these unique features of chiral edge SWs, wave splitter and interferometer functions can be realized. A 1:4 SW beam splitter using three-domain walls to conduct the edge SWs is shown in figure 7(a). SWs are split at the edge of the structure and four output beams are observed with the same amplitude. A design of the chiral edge SW interferometer is also proposed in figure 7(d). The process can be represented in the diagram in figure 7(d), which is the same as the concept of the Mach-Zehnder interferometer in optics. Topologically protected chiral edge SWs are robust against defects

J. Phys. D: Appl. Phys. **55** (2022) 123001

Topical Review

and also possess a unidirectional nature, which is promising for topological magnonic devices and circuits.

A prototype of a magnonic interferometer based on unidirectional SWs generated by nanomagnets has been proposed recently [117]. Two identical Co nanowires are patterned on top of a low-damping YIG thin film. Two beams of unidirectional exchange SWs can be excited respectively from two nanowires. Because SWs excited by two nanowires are emitted from a different position, a phase shift of $\Delta\phi = kd$ exists between two beams of SWs. When the phase shift $\Delta\phi = kd = n\pi$, where n is an odd number, two beams of SWs interfere destructively, as shown in figure 7(c). In contrast, when the phase shift $\Delta\phi = kd = n\pi$, and n is an even number, two beams of SWs interfere constructively and the SW amplitude is enhanced. The interference conditions depend on the separation distance d as well as the wavevector k. By varying these two parameters, the SW interference patterns in the frequency domain can be observed, as shown in figure 7(d). The unidirectional SW devices discussed above are mostly in the microwave regime of coherent SWs. In a very recent paper by Han *et al* nonreciprocal transmission of incoherent magnons with asymmetric diffusion lengths are found in a magnetic bilayer structure by the spin Hall effect [118]. Incoherent magnons cover the spectrum from gigahertz up to terahertz and the SW nonreciprocity can be controlled in a nonvolatile manner, which could lead to the passive directional signal isolation device in the diffusive regime.

Beyond the methods discussed above for the realization of unidirectional SW propagation, it is found that a saturation magnetization gradient of a perpendicular magnetized ferromagnetic film raises an asymmetric dispersion for nonreciprocal SW propagation [119]. Under certain circumstances, unidirectional SW propagation can also be achieved. In addition, very recently, it has been demonstrated that a simple design of a vortex core in a teardrop-shaped nano patch can serve as a unidirectional SW emitter [120].

7. Conclusions

In this review, we discuss several research developments concerning unidirectional SW propagation and devices. Unidirectional transport of electrons opens a new horizon for the electronic circuits industry. In an analogous way, the unidirectional propagation of SWs also provides a new playground in the field of magnonics. Although conventional MSSWs could host unidirectional SWs easily by enhancing the film thickness, it is difficult to use cutting-edge nanotechnology to fabricate devices that are compatible with modern nano-electronic circuits. IDMI as well as chiral spin pumping effects offer the opportunity to realize unidirectional SW propagation in nanometre-thick magnetic films, which could result in practical magnonic devices. Magnetic textures provide a new platform for the investigation of unidirectional SWs and more functionalities are expected to be explored. For example, unidirectional SWs could be channelled into a waveguide with the width of a few nanometres in a domain wall, offering more possibilities for nanomagnonic devices

and circuits. The most convenient way to control the unidirectional transport of SWs is to manipulate the external magnetic field. By switching the field direction, the unidirectionality induced by MSSWs, iDMI and chiral spin pumping effects is reversed. Unidirectional SWs can be controlled with more possibilities in reconfigurable magnetic textures. While several methods have been proposed to contribute to the realization of unidirectional SWs, the fabrication of practical, compact and low-energydissipative unidirectional SW devices is still missing. The active control of SW unidirectionality via an electric current or voltage in a magnetic system is also worth investigating in view of applications. For most cases, external magnetic fields are requisite for SWs, while the field-free efficient transport of unidirectional SWs is essential for future magnonic applications [121, 122]. It is still very challenging to realize high-speed unidirectional SW devices in the THz regime for application in antiferromagnetic magnonics [123, 124]. Furthermore, the hybrid magnonic systems such as magnon–photon [125–127] and magnon–phonon [128, 129] coupled systems also favour nonreciprocal information transport that could lead to new functional devices, circuits and coherent information processing [130]. Meanwhile, unidirectional SWs may allow new computing concepts and architectures for SWs, such as neuromorphic computing, where the information transfer between neurons via a synapse is intrinsically unidirectional [131, 132]. These unique features may trigger new spintronic devices and circuits based on unidirectional SWs.

Data availability statement

No new data were created or analysed in this study.

ORCID iDs

Jilei Chen ⬤ https://orcid.org/0000-0001-9619-8514
Haiming Yu ⬤ https://orcid.org/0000-0002-3291-6713
Gianluca Gubbiotti ⬤ https://orcid.org/0000-0002-7006-0370

References

[1] Chumak A V, Vasyuchka V I, Serga A A and Hillebrands B 2015 Magnon spintronics *Nat. Phys.* **11** 454–61
[2] Kruglyak V V, Demokritov S O and Grundler D 2010 Magnonics *J. Phys. D: Appl. Phys.* **43** 264001

J. Phys. D: Appl. Phys. **55** (2022) 123001

Topical Review

[3] Lenk B, Ulrichs H, Garbs F and Münzenberg M 2011 The building blocks of magnonics *Phys. Rep.* **507** 107–36

[4] Csaba G, Papp Á and Porod W 2017 Perspectives of using spin waves for computing and signal processing *Phys. Lett.* A **381** 1471–6

[5] Barman A *et al* 2021 The 2021 magnonics roadmap *J. Phys.: Condens. Matter* **33** 413001

[6] Demidov V E, Urazhdin S, De Loubens G, Klein O, Cros V, Anane A and Demokritov S O 2017 Magnetization oscillations and waves driven by pure spin currents *Phys. Rep.* **673** 1–31

[7] Khitun A, Bao M and Wang K L 2010 Magnonic logic circuits *J. Phys. D: Appl. Phys.* **43** 264005

[8] Neusser S and Grundler D 2009 Magnonics: spin waves on the nanoscale *Adv. Mater.* **21** 2927–32

[9] Sheng L, Chen J, Wang H and Yu H 2021 Magnonics based on thin-film iron garnets *J. Phys. Soc. Japan* **90** 081005

[10] Pirro P, Vasyuchka V I, Serga A A and Hillebrands B 2021 Advances in coherent magnonics *Nat. Rev. Mater.* 1–22

[11] Yu H, Xiao J and Schultheiss H 2021 Magnetic texture based magnonics *Phys. Rep.* **905** 1–59

[12] Han J, Zhang P, Hou J T, Siddiqui S A and Liu L 2019 Mutual control of coherent spin waves and magnetic domain walls in a magnonic device *Science* **366** 1121–5

[13] Cornelissen L J, Liu J, Duine R A, Youssef J B and Van Wees B J 2015 Long-distance transport of magnon spin information in a magnetic insulator at room temperature *Nat. Phys.* **11** 1022–6

[14] Haldar A, Kumar D and Adeyeye A O 2016 A reconfigurable waveguide for energy-efficient transmission and local manipulation of information in a nanomagnetic device *Nat. Nanotechnol.* **11** 437–43

[15] Urazhdin S, Demidov V E, Ulrichs H, Kendziorczyk T, Kuhn T, Leuthold J, Wilde G and Demokritov S O 2014 Nanomagnonic devices based on the spin-transfer torque *Nat. Nanotechnol.* **9** 509–13

[16] Madami M, Bonetti S, Consolo G, Tacchi S, Carlotti G, Gubbiotti G, Mancoff F B, Yar M A and Åkerman J 2011 Direct observation of a propagating spin wave induced by spin-transfer torque *Nat. Nanotechnol.* **6** 635–8

[17] Choudhury S, Chaurasiya A K, Mondal A K, Rana B, Miura K, Takahashi H, Otani Y and Barman A 2020 Voltage controlled on-demand magnonic nanochannels *Sci. Adv.* **6** 1–10

[18] Liu C *et al* 2019 Current-controlled propagation of spin waves in antiparallel, coupled domains *Nat. Nanotechnol.* **14** 691–7

[19] Sluka V *et al* 2019 Emission and propagation of 1D and 2D spin waves with nanoscale wavelengths in anisotropic spin textures *Nat. Nanotechnol.* **14** 328–33

[20] Hämäläinen S J, Madami M, Qin H, Gubbiotti G and Van Dijken S 2018 Control of spin-wave transmission by a programmable domain wall *Nat. Commun.* **9** 4853

[21] Demokritov S O and Slavin A N (eds) 2013 *Magnonics from Fundamentals to Applications* (Berlin: Springer)

[22] Gubbiotti G (ed) 2019 *Three-Dimensional Magnonics: Layered, Micro- and Nanostructures* (Singapore: Jenny Stanford Publishing Pte. Ltd)

[23] Rezende S M (ed) 2020 *Fundamentals of Magnonics* Lecture Notes in Physics (Switzerland: Springer) (https://doi.org/10.1007/978-3-030-41317-0)

[24] Rodríguez-Fortuño F J, Marino G, Ginzburg P, O'Connor D, Martínez A, Wurtz G A and Zayats A V 2013 Near-field interference for the unidirectional excitation of electromagnetic guided modes *Science* **340** 328–30

[25] Bi L, Hu J, Jiang P, Kim D H, Dionne G F, Kimerling L C and Ross C A 2011 On-chip optical isolation in monolithically integrated non-reciprocal optical resonators *Nat. Photon.* **5** 758–62

[26] Wang Z, Chong Y, Joannopoulos J D and Soljačić M 2009 Observation of unidirectional backscattering-immune topological electromagnetic states *Nature* **461** 772–5

[27] Landy N and Smith D R 2013 A full-parameter unidirectional metamaterial cloak for microwaves *Nat. Mater.* **12** 25–28

[28] Song A M, Missous M, Omling P, Peaker A R, Samuelson L and Seifert W 2003 Unidirectional electron flow in a nanometer-scale semiconductor channel: a self-switching device *Appl. Phys. Lett.* **83** 1881–3

[29] Fan L, Wang J, Varghese L T, Shen H, Niu B, Xuan Y, Weiner A M and Qi M 2012 An all-silicon passive optical diode *Science* **335** 447

[30] Jalas D *et al* 2013 What is—and what is not—an optical isolator *Nat. Photon.* **7** 579–82

[31] Adam J D, Krishnaswamy S V, Talisa S H and Yoo K C 1990 Thin-film ferrites for microwave and millimeter-wave applications *J. Magn. Magn. Mater.* **83** 419–24

[32] Cramer N, Lucic D, Camley R E and Celinski Z 2000 High attenuation tunable microwave notch filters utilizing ferromagnetic resonance *J. Appl. Phys.* **87** 6911–3

[33] Damon R W and Eshbach J R 1961 Magnetostatic modes of a ferromagnet slab *J. Phys. Chem. Solids* **19** 308–20

[34] Camley R E 1987 Nonreciprocal surface waves *Surf. Sci. Rep.* **7** 103–87

[35] Stancil D and Prabhakar A 2019 *Spin Waves: Theory and Applications* (Berlin: Springer)

[36] Wong K L, Bi L, Bao M, Wen Q, Chatelon J P, Lin Y-T, Ross C A, Zhang H and Wang K L 2014 Unidirectional propagation of magnetostatic surface spin waves at a magnetic film surface *Appl. Phys. Lett.* **105** 232403

[37] Sandercock J R and Wettling W 1979 Light scattering from surface and bulk thermal magnons in iron and nickel *J. Appl. Phys.* **50** 7784–9

[38] Grünberg P, Cottam M G, Vach W, Mayr C and Camley R E 1982 Brillouin scattering of light by spin waves in thin ferromagnetic films *J. Appl. Phys.* **53** 2078

[39] Hicken R J, Eley D E P, Gester M, Gray S J, Daboo C, Ives A J R and Bland J A C 1995 Brillouin light scattering studies of magnetic anisotropy in epitaxial Fe/GaAs films *J. Magn. Magn. Mater.* **145** 278–92

[40] Ganguly A K and Webb D C 1975 Microstrip excitation of magnetostatic surface waves: theory and experiment *IEEE Trans. Microw. Theory Tech.* **23** 998–1006

[41] Emtage P R 1982 Generation of magnetostatic surface waves by a microstrip *J. Appl. Phys.* **53** 5122–5

[42] Kostylev M 2013 Non-reciprocity of dipole-exchange spin waves in thin ferromagnetic films *J. Appl. Phys.* **113** 053907

[43] Gladii O, Haidar M, Henry Y, Kostylev M and Bailleul M 2016 Frequency nonreciprocity of surface spin wave in permalloy thin films *Phys. Rev.* B **93** 054430

[44] Demidov V E, Urazhdin S and Demokritov S O 2009 Control of spin-wave phase and wavelength by electric current on the microscopic scale *Appl. Phys. Lett.* **95** 262509

[45] An T *et al* 2013 Unidirectional spin-wave heat conveyer *Nat. Mater.* **12** 549–53

[46] Madami M, Khivintsev Y, Gubbiotti G, Dudko G, Kozhevnikov A, Sakharov V, Stal'makhov A, Khitun A and Filimonov Y 2018 Nonreciprocity of backward volume spin wave beams excited by the curved focusing transducer *Appl. Phys. Lett.* **113** 152403

[47] Kwon J H, Yoon J, Deorani P, Lee J M, Sinha J, Lee K J, Hayashi M and Yang H 2016 Giant nonreciprocal emission of spin waves in Ta/Py bilayers *Sci. Adv.* **2** e1501892

[48] Hillebrands B 2000 Brillouin light scattering from layered magnetic structures *Light Scattering in Solids VII* Vol 174–289 (Berlin: Springer)

[49] Carlotti G and Gubbiotti G 2002 Magnetic properties of layered nanostructures studied by Brillouin light scattering

and surface magneto-optic Kerr effect *J. Phys.: Condens. Matter* **14** 8199–233

[50] Grassi M, Geilen M, Louis D, Mohseni M, Brächer T, Hehn M, Stoeffler D, Bailleul M, Pirro P and Henry Y 2020 Slow-wave-based nanomagnonic diode *Phys. Rev. Appl.* **14** 024047

[51] Mruczkiewicz M, Graczyk P, Lupo P, Adeyeye A, Gubbiotti G and Krawczyk M 2017 Spin-wave nonreciprocity and magnonic band structure in a thin permalloy film induced by dynamical coupling with an array of Ni stripes *Phys. Rev. B* **96** 104411

[52] Gallardo R A *et al* 2019 Reconfigurable spin-wave nonreciprocity induced by dipolar interaction in a coupled ferromagnetic bilayer *Phys. Rev. Appl.* **12** 034012

[53] Moon J H, Seo S M, Lee K J, Kim K W, Ryu J, Lee H W, McMichael R D and Stiles M D 2013 Spin-wave propagation in the presence of interfacial Dzyaloshinskii-Moriya interaction *Phys. Rev. B* **88** 184404

[54] Tacchi S, Troncoso R E, Ahlberg M, Gubbiotti G, Madami M, Åkerman J and Landeros P 2017 Interfacial Dzyaloshinskii-Moriya interaction in Pt/CoFeB films: effect of the heavy-metal thickness *Phys. Rev. Lett.* **118** 147201

[55] Wang H *et al* 2020 Chiral spin-wave velocities induced by all-garnet interfacial Dzyaloshinskii-Moriya interaction in ultrathin yttrium iron garnet films *Phys. Rev. Lett.* **124** 027203

[56] Gallardo R A, Cortés-Ortuño D, Schneider T, Roldán-Molina A, Ma F, Troncoso R E, Lenz K, Fangohr H, Lindner J and Landeros P 2019 Flat bands, indirect gaps, and unconventional spin-wave behavior induced by a periodic Dzyaloshinskii-Moriya interaction *Phys. Rev. Lett.* **122** 067204

[57] Nembach H T, Shaw J M, Weiler M, Jué E and Silva T J 2015 Linear relation between Heisenberg exchange and interfacial Dzyaloshinskii-Moriya interaction in metal films *Nat. Phys.* **11** 825–9

[58] Ma X, Yu G, Razavi S A, Sasaki S S, Li X, Hao K, Tolbert S H, Wang K L and Li X 2017 Dzyaloshinskii-Moriya interaction across an antiferromagnet-ferromagnet interface *Phys. Rev. Lett.* **119** 027202

[59] Di K, Zhang V L, Lim H S, Ng S C, Kuok M H, Qiu X and Yang H 2015 Asymmetric spin-wave dispersion due to Dzyaloshinskii-Moriya interaction in an ultrathin Pt/CoFeB film *Appl. Phys. Lett.* **106** 052403

[60] Di K, Zhang V L, Lim H S, Ng S C, Kuok M H, Yu J, Yoon J, Qiu X and Yang H 2015 Direct observation of the Dzyaloshinskii-Moriya interaction in a Pt/Co/Ni film *Phys. Rev. Lett.* **114** 047201

[61] Schlitz R, Vélez S, Kamra A, Lambert C-H, Lammel M, Goennenwein S T and Gambardella P 2021 Control of nonlocal magnon spin transport via magnon drift currents *Phys. Rev. Lett.* **126** 257201

[62] Kuepferling M *et al* 2020 Measuring interfacial Dzyaloshinskii-Moriya interaction in ultrathin films (available at: http://arxiv.org/abs/2009.11830)

[63] Ma F and Zhou Y 2014 Interfacial Dzialoshinskii-Moriya interaction induced nonreciprocity of spin waves in magnonic waveguides *RSC Adv.* **4** 46454–9

[64] Chumak A V, Serga A A and Hillebrands B 2014 Magnon transistor for all-magnon data processing *Nat. Commun.* **5** 4700

[65] Ding J, Kostylev M and Adeyeye A O 2011 Magnonic crystal as a medium with tunable disorder on a periodical lattice *Phys. Rev. Lett.* **107** 047205

[66] Lee K S, Han D S and Kim S K 2009 Physical origin and generic control of magnonic band gaps of dipole-exchange spin waves in width-modulated nanostrip waveguides *Phys. Rev. Lett.* **102** 127202

[67] Topp J, Heitmann D, Kostylev M P and Grundler D 2010 Making a reconfigurable artificial crystal by ordering bistable magnetic nanowires *Phys. Rev. Lett.* **104** 207205

[68] Gubbiotti G, Tacchi S, Madami M, Carlotti G, Jain S, Adeyeye A O and Kostylev M P 2012 Collective spin waves in a bicomponent two-dimensional magnonic crystal *Appl. Phys. Lett.* **100** 162407

[69] Tacchi S, Madami M, Gubbiotti G, Carlotti G, Tanigawa H, Ono T and Kostylev M P 2010 Anisotropic dynamical coupling for propagating collective modes in a two-dimensional magnonic crystal consisting of interacting squared nanodots *Phys. Rev. B* **82** 024401

[70] Gubbiotti G, Zhou X, Haghshenasfard Z, Cottam M G and Adeyeye A O 2018 Reprogrammable magnonic band structure of layered permalloy/Cu/permalloy nanowires *Phys. Rev. B* **97** 134428

[71] Silvani R, Kuepferling M, Tacchi S and Carlotti G 2021 Impact of the interfacial Dzyaloshinskii-Moriya interaction on the band structure of one-dimensional artificial magnonic crystals: a micromagnetic study *J. Magn. Magn. Mater.* **539** 168342

[72] Mruczkiewicz M, Krawczyk M, Gubbiotti G, Tacchi S, Filimonov Y A, Kalyabin D V, Lisenkov I V and Nikitov S A 2013 Nonreciprocity of spin waves in metallized magnonic crystal *New J. Phys.* **15** 113023

[73] Yu T, Blanter Y M and Bauer G E W 2019 Chiral pumping of spin waves *Phys. Rev. Lett.* **123** 247202

[74] Yu T, Wang H, Sentef M A, Yu H and Bauer G E W 2020 Magnon trap by chiral spin pumping *Phys. Rev. B* **102** 54429

[75] Chen J *et al* 2019 Excitation of unidirectional exchange spin waves by a nanoscale magnetic grating *Phys. Rev. B* **100** 104427

[76] Wang H *et al* 2021 Tunable damping in magnetic nanowires induced by chiral pumping of spin waves *ACS Nano* **15** 9076–83

[77] Liu C *et al* 2018 Long-distance propagation of short-wavelength spin waves *Nat. Commun.* **9** 738

[78] Klingler S *et al* 2018 Spin-torque excitation of perpendicular standing spin waves in coupled YIG/Co heterostructures *Phys. Rev. Lett.* **120** 127201

[79] Qin H, Hämäläinen S J and van Dijken S 2018 Exchange-torque-induced excitation of perpendicular standing spin waves in nanometer-thick YIG films *Sci. Rep.* **8** 5755

[80] Chen J, Liu C, Liu T, Xiao Y, Xia K, Bauer G E W, Wu M and Yu H 2018 Strong interlayer magnon-magnon coupling in magnetic metal-insulator hybrid nanostructures *Phys. Rev. Lett.* **120** 217202

[81] Li Y *et al* 2020 Coherent spin pumping in a strongly coupled magnon-magnon hybrid system *Phys. Rev. Lett.* **124** 117202

[82] Shiota Y, Taniguchi T, Ishibashi M, Moriyama T and Ono T 2020 Tunable magnon-magnon coupling mediated by dynamic dipolar interaction in synthetic antiferromagnets *Phys. Rev. Lett.* **125** 017203

[83] Jiang W *et al* 2015 Blowing magnetic skyrmion bubbles *Science* **349** 283–6

[84] Kurumaji T, Nakajima T, Hirschberger M, Kikkawa A, Yamasaki Y, Sagayama H, Nakao H, Taguchi Y, Arima T-H and Tokura Y 2019 Skyrmion lattice with a giant topological Hall effect in a frustrated triangular-lattice magnet *Science* **365** 914–8

[85] Mühlbauer S, Binz B, Jonietz F, Pfleiderer C, Rosch A, Neubauer A, Georgii R and Böni P 2009 Skyrmion lattice in a chiral magnet *Science* **323** 915–9

J. Phys. D: Appl. Phys. **55** (2022) 123001

Topical Review

[86] Yu X Z, Onose Y, Kanazawa N, Park J H, Han J H, Matsui Y, Nagaosa N and Tokura Y 2010 Real-space observation of a two-dimensional skyrmion crystal *Nature* **465** 901–4

[87] Woo S *et al* 2016 Observation of room-temperature magnetic skyrmions and their current-driven dynamics in ultrathin metallic ferromagnets *Nat. Mater.* **15** 501–6

[88] Wang Z *et al* 2020 Thermal generation, manipulation and thermoelectric detection of skyrmions *Nat. Electron.* **3** 672–9

[89] Maccariello D, Legrand W, Reyren N, Garcia K, Bouzehouane K, Collin S, Cros V and Fert A 2018 Electrical detection of single magnetic skyrmions in metallic multilayers at room temperature *Nat. Nanotechnol.* **13** 233–7

[90] Saha S *et al* 2019 Formation of Neél-type skyrmions in an antidot lattice with perpendicular magnetic anisotropy *Phys. Rev.* B **100** 144435

[91] Nayak A K, Kumar V, Ma T, Werner P, Pippel E, Sahoo R, Damay F, Rößler U K, Felser C and Parkin S S P 2017 Magnetic antiskyrmions above room temperature in tetragonal Heusler materials *Nature* **548** 561–6

[92] Litzius K *et al* 2017 Skyrmion Hall effect revealed by direct time-resolved x-ray microscopy *Nat. Phys.* **13** 170–5

[93] Parkin S S P, Hayashi M and Thomas L 2008 Magnetic domain-wall racetrack memory *Science* **320** 190–4

[94] Allwood D A, Xiong G, Faulkner C C, Atkinson D, Petit D and Cowburn R P 2005 Magnetic domain-wall logic *Science* **309** 1688–92

[95] Caretta L *et al* 2018 Fast current-driven domain walls and small skyrmions in a compensated ferrimagnet *Nat. Nanotechnol.* **13** 1154–60

[96] Haazen P P J, Murè E, Franken J H, Lavrijsen R, Swagten H J M and Koopmans B 2013 Domain wall depinning governed by the spin Hall effect *Nat. Mater.* **12** 299–303

[97] Luo Z, Hrabec A, Dao T P, Sala G, Finizio S, Feng J, Mayr S, Raabe J, Gambardella P and Heyderman L J 2020 Current-driven magnetic domain-wall logic *Nature* **579** 214–8

[98] Garcia-Sanchez F, Borys P, Soucaille R, Adam J P, Stamps R L and Kim J V 2015 Narrow magnonic waveguides based on domain walls *Phys. Rev. Lett.* **114** 247206

[99] Wagner K, Kákay A, Schultheiss K, Henschke A, Sebastian T and Schultheiss H 2016 Magnetic domain walls as reconfigurable spin-wave nanochannels *Nat. Nanotechnol.* **11** 432–6

[100] Chang L J *et al* 2020 Spin wave injection and propagation in a magnetic nanochannel from a vortex core *Nano Lett.* **20** 3140–6

[101] Li Z, Dong B, He Y, Chen A, Li X, Tian J H and Yan C 2021 Propagation of spin waves in a 2D vortex network *Nano Lett.* **21** 4708–14

[102] Henry Y, Stoeffler D, Kim J V and Bailleul M 2019 Unidirectional spin-wave channeling along magnetic domain walls of Bloch type *Phys. Rev.* B **100** 024416

[103] Chen J, Hu J and Yu H 2020 Chiral magnonics: reprogrammable nanoscale spin wave networks based on chiral domain walls *iScience* **23** 101153

[104] Seki S, Garst M, Waizner J, Takagi R, Khanh N D, Okamura Y, Kondou K, Kagawa F, Otani Y and Tokura Y 2020 Propagation dynamics of spin excitations along skyrmion strings *Nat. Commun.* **11** 256

[105] Yokouchi T *et al* 2018 Current-induced dynamics of skyrmion strings *Sci. Adv.* **4** eaat1115

[106] Iwasaki J, Beekman A J and Nagaosa N 2014 Theory of magnon-skyrmion scattering in chiral magnets *Phys. Rev.* B **89** 064412

[107] Van De Wiele B, Hämäläïnen S J, Baláz P, Montoncello F and Van Dijken S 2016 Tunable short-wavelength spin wave excitation from pinned magnetic domain walls *Sci. Rep.* **6** 21330

[108] Holländer R B, Müller C, Schmalz J, Gerken M and McCord J 2018 Magnetic domain walls as broadband spin wave and elastic magnetisation wave emitters *Sci. Rep.* **8** 13871

[109] Albisetti E *et al* 2020 Optically inspired nanomagnonics with nonreciprocal spin waves in synthetic antiferromagnets *Adv. Mater.* **32** 1906439

[110] Albisetti E *et al* 2016 Nanopatterning reconfigurable magnetic landscapes via thermally assisted scanning probe lithography *Nat. Nanotechnol.* **11** 545–51

[111] Díaz S A, Hirosawa T, Loss D and Psaroudaki C 2020 Spin wave radiation by a topological charge dipole *Nano Lett.* **20** 6556–62

[112] Chen J, Hu J and Yu H 2021 Chiral emission of exchange spin waves by magnetic skyrmions *ACS Nano* **15** 4372–9

[113] Lan J, Yu W, Wu R and Xiao J 2015 Spin-wave diode *Phys. Rev. X* **5** 041049

[114] Szulc K, Graczyk P, Mruczkiewicz M, Gubbiotti G and Krawczyk M 2020 Spin-wave diode and circulator based on unidirectional coupling *Phys. Rev. Appl.* **14** 034063

[115] Shindou R, Matsumoto R, Murakami S and Ohe J I 2013 Topological chiral magnonic edge mode in a magnonic crystal *Phys. Rev.* B **87** 174427

[116] Wang X S, Zhang H W and Wang X R 2018 Topological magnonics: a paradigm for spin-wave manipulation and device design *Phys. Rev. Appl.* **9** 024029

[117] Chen J *et al* 2021 Reconfigurable spin-wave interferometer at the nanoscale *Nano Lett.* **21** 6237–44

[118] Han J, Fan Y, McGoldrick B C, Finley J, Hou J T, Zhang P and Liu L 2021 Nonreciprocal transmission of incoherent magnons with asymmetric diffusion length *Nano Lett.* **21** 7037–43

[119] Borys P, Kolokoltsev O, Qureshi N, Plumer M L and Monchesky T L 2021 Unidirectional spin wave propagation due to a saturation magnetization gradient *Phys. Rev.* B **103** 144411

[120] Osuna Ruiz D, Martin E L, Hibbins A P and Ogrin F Y 2021 Unidirectional emission and reconfigurability of channeled spin waves from a vortex core in a teardrop-shaped nanopatch *Phys. Rev.* B **104** 094427

[121] Haldar A, Tian C and Adeyeye A O 2017 Isotropic transmission of magnon spin information without a magnetic field *Sci. Adv.* **3** e1700638

[122] Qin H, Dreyer R, Woltersdorf G, Taniyama T and Van Dijken S 2021 Electric-field control of propagating spin waves by ferroelectric domain-wall motion in a multiferroic heterostructure *Adv. Mater.* **2100646** 1–9

[123] Hortensius J R, Afanasiev D, Matthiesen M, Leenders R, Citro R, Kimel A V, Mikhaylovskiy R V, Ivanov B A and Caviglia A D 2021 Coherent spin-wave transport in an antiferromagnet *Nat. Phys.* **17** 1001–6

[124] Kampfrath T, Sell A, Klatt G, Pashkin A, Mährlein S, Dekorsy T, Wolf M, Fiebig M, Leitenstorfer A and Huber R 2011 Coherent terahertz control of antiferromagnetic spin waves *Nat. Photon.* **5** 31–34

[125] Wang Y P, Rao J W, Yang Y, Xu P C, Gui Y S, Yao B M, You J and Hu C-M 2019 Nonreciprocity and unidirectional invisibility in cavity magnonics *Phys. Rev. Lett.* **123** 127202

[126] Hou J T and Liu L 2019 Strong coupling between microwave photons and nanomagnet magnons *Phys. Rev. Lett.* **123** 107702

[127] Li Y *et al* 2019 Strong coupling between magnons and microwave photons in on-chip ferromagnet-

superconductor thin-film devices *Phys. Rev. Lett.*
123 107701

[128] Xu M, Yamamoto K, Puebla J, Baumgaertl K, Rana B,
Miura K, Takahashi H, Grundler D, Maekawa S and
Otani Y 2020 Nonreciprocal surface acoustic wave
propagation via magneto-rotation coupling *Sci. Adv.*
6 eabb1724

[129] Kü M, Heigl M, Flacke L, Hörner A, Weiler M, Albrecht M
and Wixforth A 2020 Nonreciprocal
Dzyaloshinskii-Moriya magnetoacoustic waves *Phys. Rev.
Lett.* **125** 217203

[130] Li Y, Zhang W, Tyberkevych V, Kwok W K, Hoffmann A
and Novosad V 2020 Hybrid magnonics: physics, circuits,
and applications for coherent information processing
J. Appl. Phys. **128** 130902

[131] Torrejon J *et al* 2017 Neuromorphic computing with
nanoscale spintronic oscillators *Nature* **547** 428–31

[132] Zahedinejad M, Awad A A, Muralidhar S, Khymyn R,
Fulara H, Mazraati H, Dvornik M and Åkerman J 2020
Two-dimensional mutually synchronized spin Hall
nano-oscillator arrays for neuromorphic computing *Nat.
Nanotechnol.* **15** 47–52